A R C H I V E S O F M E T A L L U R G Y A N D M A T E R I A L S
Volume 53 2008 Issue 4

C. HAMILTON*, S. DYMEK**, M. BLICHARSKI**

FRICTION STIR WELDING OF ALUMINUM 7136-T76511 EXTRUSIONS

ZGRZEWANIE TARCIOWE Z MIESZANIEM MATERIAŁU ZGRZEINY STOPU ALUMINUM 7136-T76511

This research program evaluates the residual properties of 7136-T76511 aluminum extrusions joined through friction stir welding (FSW). The 7136 alloy is a new aluminum alloy developed by Universal Alloy Corporation for high strength aerospace applications that also demand good corrosion resistance, such as those on the Boeing 787 or the Airbus A380. Testing was performed on the baseline material and on panels friction stir welded at 175, 225, 250, 300, 350 and 400 rotation per minute (all other welding parameters were held constant). Mechanical properties correlated with the energy per unit length of weld, i.e. the highest joint efficiency, 74% (based on tensile strength, R_m), was achieved at the highest welding energy. For each weld condition, the elongation of the welded material is significantly reduced, 50 – 75%, from the baseline value. Fracture of the tensile specimens consistently occurred on the retreating side of the weld along the interface between the heat affected zone (HAZ) and the thermo-mechanically affected zone (TMAZ), independent of the rotational speed. Examination of fracture surfaces through SEM revealed nucleation and growth of microvoids around secondary phase particles present in the microstructure.

Keywords: friction stir welding, aluminum, microstructure, mechanical properties

W badaniach wyznaczono podstawowe własności mechaniczne stopu aluminium 7136-T76511 poddanego zgrzewaniu metodą tarciową z mieszaniem materiału zgrzeiny (*Friction Stir Welding*). Stop 7136 jest nowym stopem aluminium zaprojektowanym i wytwarzanym przez Universal Alloy Corporation (USA) wykazującym wysoką wytrzymałość i dobrą odporność korozyjną. Stop ten, przeznaczony głównie do zastosowań w lotnictwie, znalazł już zastosowanie w samolotach Boeing 787 oraz Airbus A380. Próbę rozciągania przeprowadzono na próbkach z materiału rodzimego oraz zawierającego zgrzeinę. Zgrzeiny wykonywano przy różnych szybkościach obrotowych narzędzia: 175, 225, 250, 300, 350 i 400 obr/min (wszystkie inne parametry procesu nie ulegały zmianie). Największą "efektywność połączenia" mierzoną stosunkiem wytrzymałości R_m połączenia do R_m materiału rodzimego w odniesieniu do dostarczonej energii (na jednostkę długości zgrzeiny), 74%, otrzymano dla największej energii zgrzewania. Dla wszystkich warunków zgrzewania wydłużenie próbek ulegało znacznemu obniżeniu, 50 – 75% wydłużenia materiału rodzimego. Pękanie próbek podczas rozciągania zachodziło zawsze po stronie spływu (cofania) materiału wzdłuż granicy pomiędzy strefą wpływu ciepła a strefą poddaną procesom cieplno-mechanicznym, niezależnie od szybkości obrotu narzędzia. Badania powierzchni przełomów wykazały obecność mikropustek, których zarodkowanie i wzrost zachodziły na wtrąceniach.

1. Introduction

As the aerospace industry produces new and more efficient airframes, the need to provide high-strength, lightweight alloys that meet the more aggressive design objectives for mechanical performance, manufacturability and service life arises. To that end, the aluminum industry, in particular the extrusion mills, have sought to develop alloys and heat treatments that combine superior mechanical properties with excellent resistance to exfoliation corrosion and stress corrosion cracking. One such alloy and temper combination is 7136-T76511, an alloy produced by the Universal Alloy Corporation (UAC) based in Anaheim, CA, USA. Because of its superior mechanical performance and corrosion resistance, 7136-T76511 extrusions are very attractive to airframe designers seeking to reduce weight in order to increase fuel efficiency and aerodynamic performance and also trying to extend the service life by introducing alloys more resistant to corrosion. Both Airbus and Boeing uti-

* MIAMI UNIVERSITY, DEPARTMENT OF MECHANICAL AND MANUFACTURING ENGINEERING, KREGER HALL, OXFORD, OH 45056, USA
** AGH UNIVERSITY OF SCIENCE AND TECHNOLOGY, FACULTY OF METALS ENGINEERING AND INDUSTRIAL COMPUTER SCIENCE, 30-059 KRAKÓW, 30 MICKIEWICZA AV., POLAND

lize 7136-T76511 extrusions on their new airplanes, the A380 and the 787.

Aluminum 7136 contains higher levels of zinc than typical 7XXX alloys (8.4 – 9.4 wt%) and primarily utilizes chromium (0.05 wt%) to control grain growth and recrystallization, akin to the popular 7075 chemistry. The alloy, however, also contains zirconium (0.10 – 0.20 wt%) as a microstructural modifier, similar to the 7X5X family of alloys (the chemical composition of aluminum 7136 is summarized in Table 1 [1]). Produced in a conventional, i.e. the heat treatment is not patented or proprietary to the supplier, - T76511 temper, 7136 offers superior mechanical properties to 7075-T6511 with an excellent and guaranteed exfoliation corrosion rating of EB per ASTM G 34 standard.

TABLE 1

Chemical composition of aluminium 7136

Element	Weight Percent	
	Minimum	Maximum
Zn	8.4	9.4
Mg	1.8	2.5
Cu	1.9	2.5
Zr	0.10	0.20
Fe	–	0.15
Si	–	0.12
Ti	–	0.10
Mn	–	0.05
Cr	–	0.05
Other, Each	0.05	
Other, Total	0.15	
Al	Remainder	

The impact of friction stir welding (FSW) on the structure and properties of 7136-T76511 is of primary importance. Invented in 1991 by The Welding Institute, friction stir welding is a novel solid-state joining process that is gaining popularity in the manufacturing sector [2, 3]. FSW utilizes a rotating tool design to induce plastic flow in the base metals and essentially "stirs" the pieces together. During the welding process, a pin, attached to the primary tool, is inserted into the joint with the shoulder of the rotating tool abutting the base metals. As the tool traverses the joint, the rotation of the shoulder under the influence of an applied load heats the metal surrounding the joint and with the rotating action of the pin induces metal from each workpiece to flow and form the weld. The microstructure resulting from the influence of plastic deformation and elevated temperature is characterized by a central weld nugget surrounded by a thermo-mechanically affected zone (TMAZ) and heat affected zone (HAZ). The welded joint is fundamentally defect-free and displays excellent mechanical properties when compared to conventional fusion welds [4 – 7]. Over the last fifteen years, numerous investigations have sought to characterize the principles of FSW and to model the microstructural evolution. The current status of FSW research has been well summarized by M i s h r a and M a [8]. Since no melting occurs during FSW, the process is performed at much lower temperatures than conventional welding techniques and circumvents many of the environmental and safety issues associated with these welding methods. In addition, due to these benefits, the aerospace industry is embracing FSW technology and implementing new welding capabilities into their manufacturing sectors.

The goal of this research was to characterize the mechanical behavior of 7136-T76511 extrusions joined by friction stir welding conducted at different rotation speeds and its correlation with an energy expenditure per unit length of weld. To identify the optimum weld condition, the evaluation of joint efficiency (defined here as the ratio of tensile strength of the weld and base material) was estimated for particular rotation speeds.

2. Experimental procedure

2.1. Friction stir welding

Aluminum 7136-T76511 extrusions produced in accordance with an internal specification from UAC with a thickness of 6.35 mm and a width of 101.6 mm were obtained and welded by the Edison Welding Institute

(EWI, Columbus, OH) in the butt-weld configuration represented in Figure 1. As shown in the diagram, FSW occurs along the L-direction of the extrusions with a clockwise tool rotation. On the advancing side of the weld, rotation of the tool is in the same direction as the weld direction, but on the retreating side, rotation of the tool is in the opposite direction of the weld direction (the advancing and retreating sides are indicated in the figure). The diameter of the FSW tool shoulder was 17.8 mm, the pin diameter tapered linearly from 10.3 mm at the tool shoulder to 7.7 mm at the tip and the pin depth was 6.1 mm. More specific details of the tool design are proprietary to EWI, but Mishra and Ma have reviewed many of the common FSW tool designs that are indicative of that utilized in this investigation [8]. With a constant weld velocity of 2.1 mm/s and a constant applied force of 26.7 kN, unique welds were produced at the following tool rotation speeds: 175, 225, 250, 300, 350 and 400 rotation per minute (RPM). The microstructure of all welds was uniform without any voids and other inhomogeneities (Fig. 2). In particular, no characteristic "nugget", found in other works [7, 8] was observed.

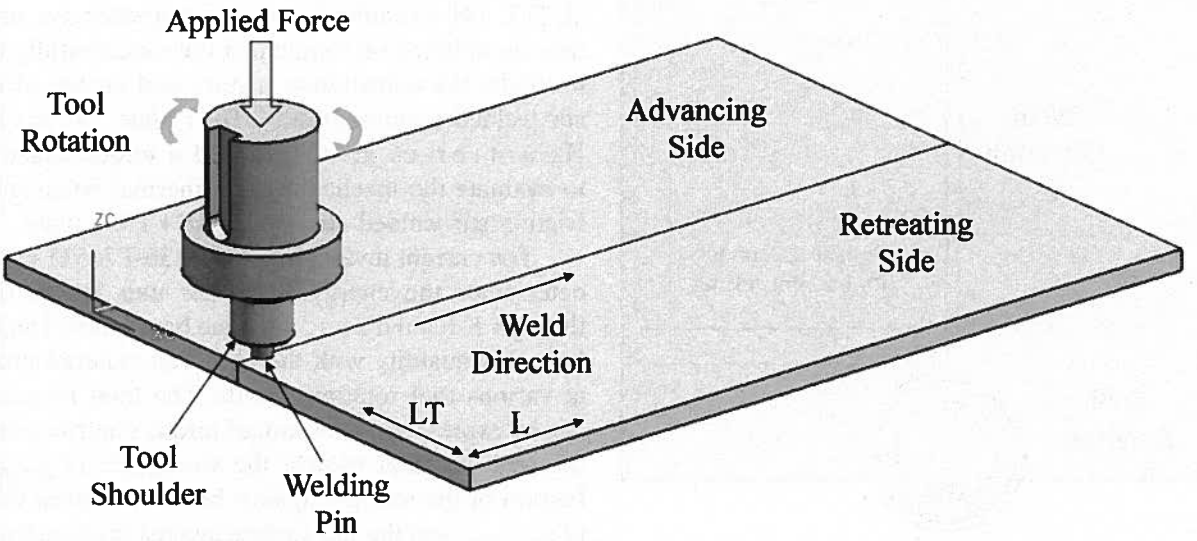

Fig. 1. Schematic of butt-weld geometry and FSW orientation

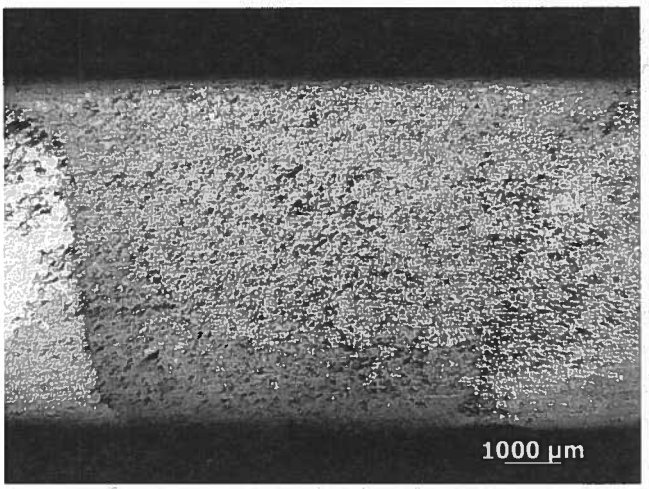

Fig. 2. Typical microstructure of the weld produced at 250 RPM

2.2. Mechanical testing

From the welded panels of each tool rotation speed, full thickness (6.35 mm) tensile samples were excised perpendicular to the friction stir weld with the weld, itself, centered along the tensile specimen in the reduced section, as shown in Figure 3. In this orientation, the load is applied transverse to the weld direction and across all microstructural regions associated with the welding process, i.e. weld nugget, HAZ and TMAZ. In addition to the welded tensile specimens, tensile bars of the same geometry and dimensions were also excised from an area well away from the weld region for baseline property comparison. All tensile tests were performed in accordance with ASTM E 8 utilizing an Instron 5867 screw driven test frame with a 30 kN load cell and a 0.001 – 500 mm/min speed range. Specimen extension, crosshead deflection and load were recorded throughout the test duration. Specimen extension was measured by means of an extensometer attached to the reduced section that spanned the width of the weld. The extensometer remained attached to the specimen through yielding, but was removed prior to specimen failure to prevent damage to the equipment. The yield strength was obtained by the 0.2% offset method ($R_{p0.2}$) and the elongation, e, was determined by scribing marks with known sep-

aration within the reduced section prior to testing and measuring their separation after testing.

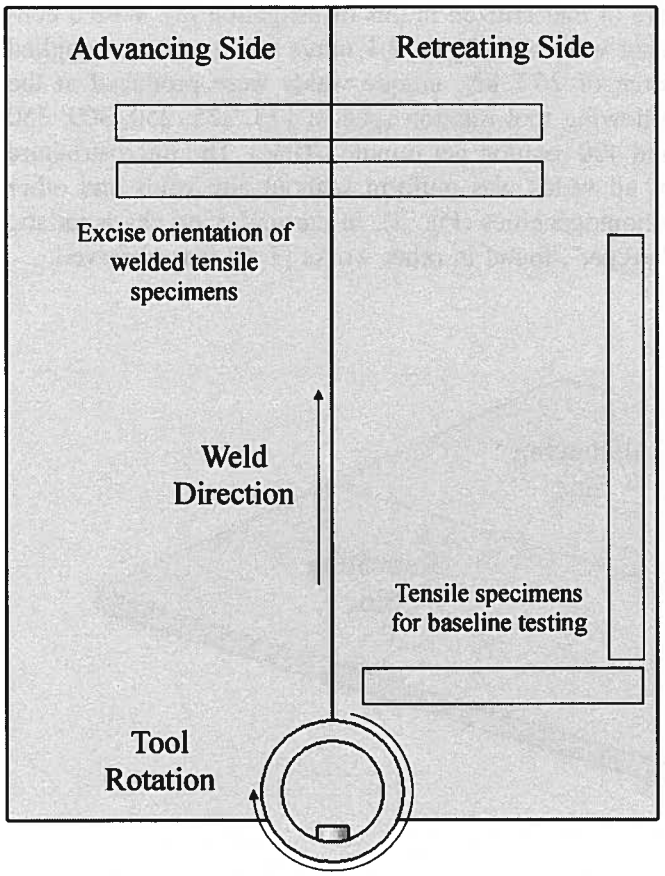

Fig. 3. Excise location of tensile specimens and corrosion coupons from FSW panels

3. Results and discussion

3.1. Mechanical properties

Six different tool rotation speeds were examined in order to assess the impact of changing weld parameters on the mechanical properties and to identify the optimum weld condition leading to the highest joint efficiency. Since the weld velocity and the applied force were held constant during FSW and only the tool rotation speed was varied, the tool RPM does provide a relative measure of the energy imparted into the aluminum extrusions due to changes in the process parameters. It is, however, more appropriate to evaluate the influence of the process parameters, weld velocity (v_w), tool rotation speed (ω) and applied force (F), during friction stir welding in terms of the total heat or energy imparted to the work pieces during welding, rather than the impact of a single parameter. Since varying any of the identified parameters changes the heat input of the system, correlating the heat input with the resultant material behavior gives greater insight into the friction stir welding process.

To that end, Arbegast et al. [11] defined the pseudo-heat index as the ratio of the square of the angular velocity (rotation speed) and the weld velocity, i.e. ω^2/v_w, as a quantitative assessment of the heat input during FSW. On the other hand, Ren et al. [12] have simply utilized the weld ratio, ω/v_w, as a measure of the heat index. During their study of aluminum 6061-T651 plate, however, Ren et. al determined that neither the pseudo-heat index or the weld ratio could be successfully correlated with the observed mechanical properties or fracture behavior. Khandkar et al. [13, 14] introduced a more comprehensive model of heat input based on torque that they successfully utilized to model the temperature history and profile of friction stir welded aluminum 6061-T651 plate. Similarly, Heurtier et. al [15] utilized a torque based model to evaluate the mechanical and thermal behavior of the friction stir welded aluminum 2024-T351 plate.

The current investigation of 7136-T76511 extrusions determines the energy input per unit length of weld through Khandkar's torque based model and correlates this quantity with the observed material properties at various tool rotation speeds. The total torque, T_{total}, can be expressed as the sum of torque contributions from the tool shoulder against the workpiece ($T_{shoulder}$), the bottom of the tool pin against bottom material thickness ($T_{pinbottom}$) and the pin surface against thickness material ($T_{pinsurface}$), such that:

$$T_{total} = T_{shoulder} + T_{pinbottom} + T_{pinsurface}. \quad (1)$$

Introducing τ as the shear stress during welding, then the total torque becomes:

$$T_{total} = \int_{r_{i1}}^{r_o} (\tau r)(2\pi r)dr + \int_{0}^{r_{i2}} (\tau r)(2\pi r)dr + 2\pi\tau r_i^2 h, \quad (2)$$

where r_o is the radius of the tool shoulder, r_{i1} is the radius of the pin at the tool shoulder, r_{i2} is the radius of the pin at the pin bottom and h is the pin height. To simply the evaluation of Equation 2, the taper of the welding pin is ignored, i.e. $r_{i1} = r_{i2} = r_i$, thus

$$T_{total} = \tau(\frac{2}{3}\pi r_o^3 + 2\pi r_i^2 h) = 2\mu F(\frac{r_o}{3} + \frac{r_i^2}{r_o^2}h), \quad (3)$$

where F is the applied force and μ is the coefficient of friction between the tool and the extrusions. The energy per unit length of weld, E_l, is found by dividing the average power, P_{avg}, by the weld velocity to ultimately yield the expression in Equation 5:

$$P_{avg} = T_{total}\omega \tag{4}$$

$$E_l = \frac{P_{avg}}{v_w} = T_{total}\frac{\omega}{v_w}. \tag{5}$$

Though the applied force during FSW was set at 26.7 kN, real time data from the welding trials revealed that the load oscillated as the machine continuously corrected the load toward the set point. Consequently, the average load during welding deviated from the desired set point; therefore, the average load was determined from the recorded data for each weld condition and was utilized in the analysis of that condition. The recorded data did verify that the weld velocity remained constant at 2.1 mm/s for all welding trials. Using a coefficient of sliding friction between aluminum and mild steel of 0.47 [16], Table 2 summarizes the average mechanical properties and the energy per unit length of weld determined for each tool rotation speed. The baseline material, in both the L and LT orientations, displayed tensile strengths in excess of 635 MPa. Most notable is that the maximum joint efficiency, 74.6%, is obtained at the highest energy level of 1768 J/mm, corresponding to 350 RPM. Under this condition, not only is the highest tensile strength obtained, but the yield strength and elongation are also greater than those of the other weld conditions. In contrast, the conditions corresponding to 175 RPM produced the lowest joint efficiency, 69.1%, which is obtained at the lowest energy level of 810 J/mm.

TABLE 2

Summary of energy and mechanical properties for each weld condition

RPM	Load (kN)	E_l (J/mm)	R_m (MPa)	$R_{p0.2}$ (MPa)	e (%)	Eff. (%)
L	–	–	641	614	10.5	–
LT	–	–	635	607	10.9	–
175	24.3	810	443	354	5.5	69.1
225	29.0	1245	449	354	5.3	70.0
250	20.9	997	448	340	4.1	69.9
300	29.4	1684	465	355	5.2	72.5
350	26.5	1768	478	362	6.6	74.6
400	21.1	1606	454	352	5.4	70.8

Figure 4 displays the relationship between the strength properties and the energy/length. For the tensile strength, a correlation with the energy/length is revealed for which the tensile strength increases with increasing energy/length. For energy levels corresponding to 175, 250 and 225 RPM, the tensile strength appears somewhat insensitive to the energy/length as the tensile strength rises only 6 MPa as the energy increases from 810 J/mm to 1245 J/mm. For energy levels corresponding to 400, 300 and 350 RPM, the tensile strength is more sensitive to the energy level with the tensile strength rising 24 MPa as the energy increases from 1684 J/mm to 1768 MPa. If each of these data sets represents a distinct region of material behavior, then an energy/length of 1600 J/mm marks the transition between the two regimes. It is significant to note that correlating the tensile strength with the weld ratio [11] or the pseudo-heat index [12] would have masked this relationship and simply shown a local maximum occurring at 350 RPM. As suggested by Ren et al. [12], these welding parameters are not suitable for correlating welding conditions with mechanical properties. The relationship between the yield strength and the energy/length, however, is not as clearly defined, though the highest yield strength is still achieved at the highest energy level examined. For energy levels corresponding to 175, 250 and 225 RPM, the yield strength appears insensitive to the energy, showing no net increase as the energy level rises from 810 J/mm to 1245 J/mm. For energy levels corresponding to 400, 300 and 350 RPM, however, the yield strength, much like the tensile strength, rises sharply (10 MPa) over a 84 J/mm increase in energy.

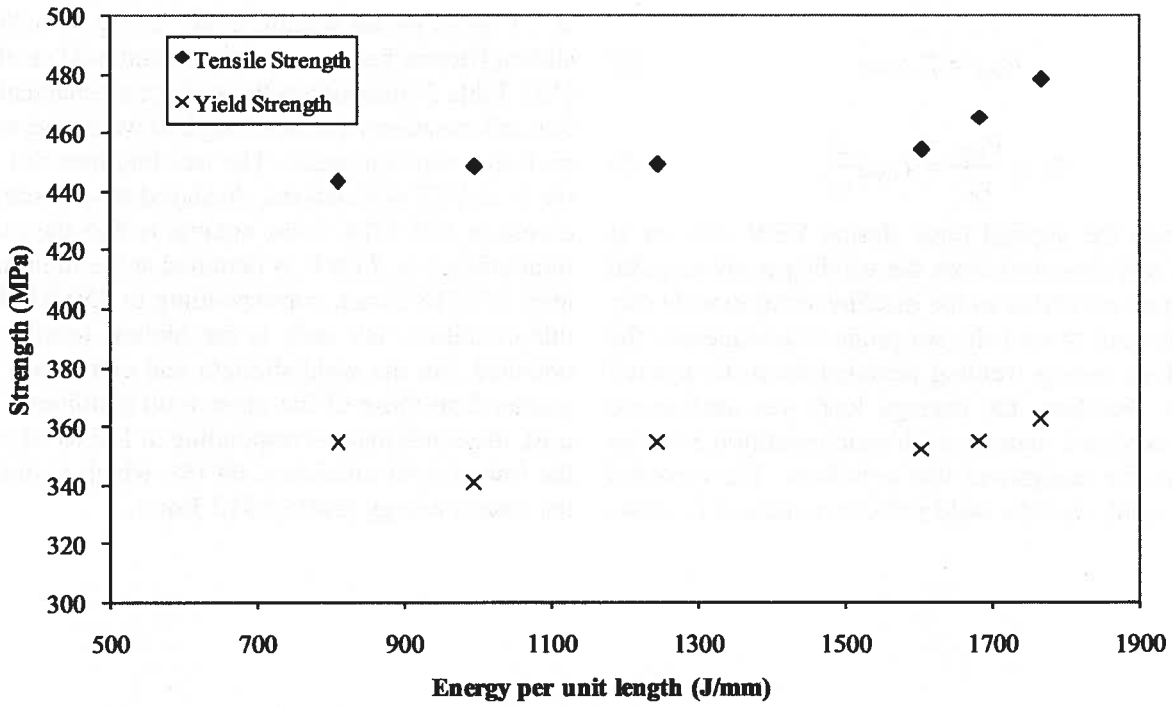

Fig. 4. Ultimate and yields strengths as a function of the energy per unit length of weld

Since the energy/length is an indication of the welding temperature, the relationship between the mechanical properties and energy/length suggests that a similar relationship must exist between the mechanical properties and the welding temperature. It is well known that the temperature has a great impact on microstructure of age-hardenable Al alloys. As the energy rises, the welding temperatures will also increase, and the highest welding temperatures will occur directly beneath the tool shoulder. A comprehensive computational fluid dynamics model by Sato et al. confirms this assertion and demonstrates that typical welding temperatures under the tool shoulder and around the pin can exceed 500°C, temperatures sufficient to solution heat treat 7136 (aluminum 7136-T76511 extrusions are solution heat treated at 471°C) and dissolve the strengthening phases [17]. The increase in mechanical properties that begins at 1600 J/mm, therefore, may be due to the partial dissolution of the hardening phases under the tool and re-precipitation of these phases after the tool passes and the work pieces cool. The degree of dissolution/re-precipitation will increase with increasing energy input and will display the greatest sensitivity near the solution temperature.

3.2. Fracture behavior

Fracture surfaces from baseline tensile specimens, both L and LT, displayed ductile rupture as the primary failure mechanism. Figure 5a shows a typical baseline, 7136-T76511 fracture surface and reveals the microvoid growth around the secondary phase particles. An unusual characteristic of this fracture surface are the facets of cleavage fracture that are also present. Though this behavior is not normally associated with aluminum alloys, it is commonly observed in other high strength aluminum alloy extrusions, such as 7150-T77511 [18]. In these high strength extrusions, the heat treatment that ultimately combines mechanical performance and corrosion resistance promotes a high density of strengthening participates within the grains, and the grains, themselves, become significantly oriented during the extrusion process. The resulting fracture surface is primarily characterized by ductile rupture with laminar facets coincident to the LT orientation.

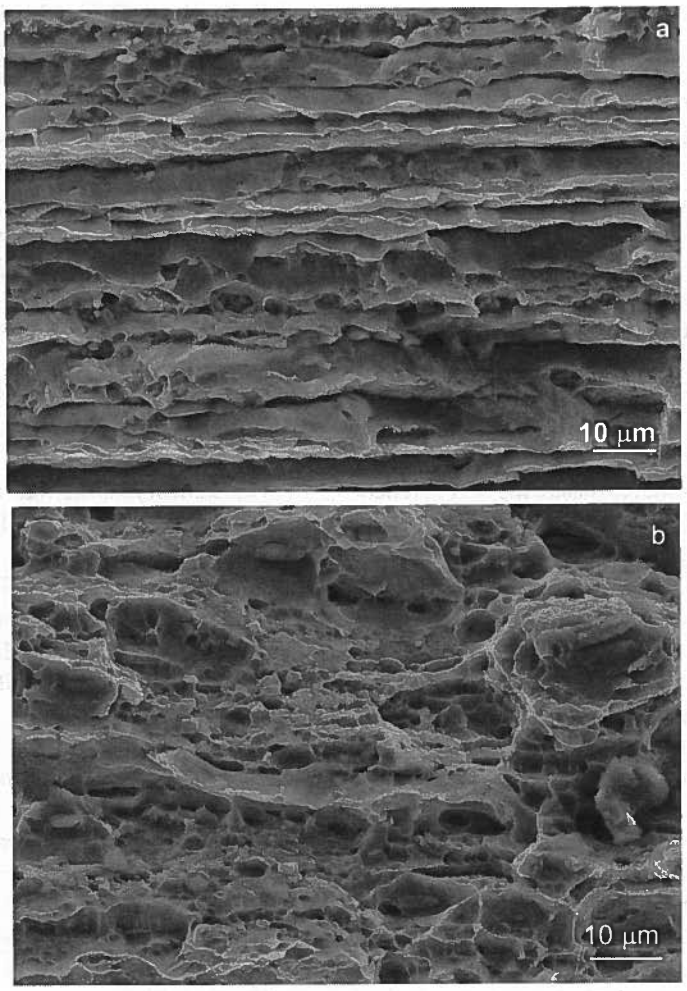

Fig. 5. Representative fracture surface: (a) baseline and (b) friction stir welded

All welded tensile specimens, regardless of the tool rotation speed, fractured on the retreating side of the weld at the interface between the TMAZ and HAZ. The fracture path initiated at the top surface, i.e. the surface of tool contact, of the tensile specimens, approximately 9 mm (the radius of the tool shoulder) from the weld centerline. Tensile failure on the retreating side is a common phenomenon in friction stir welding, just as other research studies on aluminum alloys 6063-T5, 6061-T6, 6101-T6 and 7075-T651 have also observed [7, 19, 20]. As with the baseline specimens, the fracture surfaces of the welded specimens are primarily characterized by ductile rupture, as the representative fracture surface in Figure 5b shows.

4. Conclusions

1. Mechanical testing revealed that the highest joint efficiency occurred at an energy level of 1768 J/mm, corresponding to 350 rotation per minute. The correlation between the mechanical properties and the energy/length demonstrates that the tensile strength is relatively insensitive to energy levels below 1600 J/mm, but rises sharply with energy levels beyond this threshold.
2. Since the energy/length is indicative of the welding temperature, the correlation of tensile strength with the welding energy is related to the re-precipitation and aging of strengthening phases under the tool shoulder as the welding temperature approaches the solution heat treat temperature of the alloy.
3. Examination of fracture surfaces for weld conditions reveals ductile rupture as the primary failure mechanism. Rupture of the tensile specimens consistently occurred along the retreating side of the weld at the interface between the heat affected zone and thermo-mechanically affected zone.

Acknowledgements

This research was financially supported by AGH University of Science and Technology, project no. 11.11.110.792.

REFERENCES

[1] I. Gheorghe, D. Malejan, Universal Alloy Corporation, Anaheim, CA, 2006.

[2] W. M. Thomas et al., Great Britain Patent Application No. 9125978.8 (December 1991).

[3] C. Dawes, W. Thomas, TWI Bulletin 6, p. 124 November/December 1995, p. 124.

[4] M. A. Sutton, B. C. Yang, A. P. Reynolds, J. H. Yan, Banded microstructure in 2024-T351 and 2524-T351 aluminum friction stir welds – Part II. Mechanical characterization, Materials Science and Engineering A-Structural Materials Properties Microstructure and Processing, vol. 364, pp. 66-74, 2004 (CD ROM).

[5] B. J. Dracup, W. J. Arbegast, Proceedings of the 1999 SAE Aerospace Automated Fastening Conference & Exposition, Memphis, TN, October 5-7, 1999.

[6] A. von Strombeck, J. F. dos Santos, F. Torster, P. Laureano, M. Kocak, Proceedings of the First International Symposium on Friction Stir Welding, Thousand Oaks, CA, USA, June 14-16, 1999 (CD ROM).

[7] C. Hamilton, S. Dymek, M. Blicharski, Comparison Of Mechanical Properties For 6101-T6 Extrusions Welded By Friction Stir Welding And Metal Inert Gas Welding, Archives of Metallurgy and Materials, **52**, 67, (2007).

[8] R. S. Mishra, Z. Y. Ma, Friction stir welding and processing, Materials Science & Engineering R-Reports **50**, III-78 (2005).

[9] W. M. Thomas, E. D. Nicholas, S. D. Smith, S. K. Das, J. G. Kaufman, T. J. Lienert (Eds.), Aluminum 2001 – Proceedings of the TMS 2001 Aluminum Automotive and Joining Sessions, p. 213, 2001.

[10] W. M. Thomas, K. I. Johnson, C. S. Wiesner, Friction stir welding-recent developments in tool and process technologies, Advanced Engineering Materials **5**, 485-490 (2003).

[11] W. J. Arbegast, Z. Jin, A. Beaudoin, T. A. Bieler, B. Radhakrishnan (Eds.), Hot Deformation of Aluminum Alloys III, TMS, Warrendale, PA, USA, p. 313 (2003).

[12] S. R. Ren, Z. Y. Ma, L. Q. Chen, Effect of welding parameters on tensile properties and fracture behavior of friction stir welded Al-Mg-Si alloy, Scripta Materialia **56**, 69-72, (2007).

[13] M. Z. H. Khandkar, J. A. Khan, A. P. Reynolds, Prediction of temperature distribution and thermal history during friction stir welding: input torque based model, Science and Technology of Welding and Joining, **8**, 165-174 (2003).

[14] M. Z. H. Khandkar, J. A. Khan, A. P. Reynolds, M. A. Sutton, Predicting residual thermal stresses in friction stir welded metals, Journal of Materials Processing Technology **174**, 195-203 (2006).

[15] P. Heurtier, M. J. Jones, C. Desrayaud, J. H. Driver, F. Montheillet, D. Allehaux, Mechanical and thermal modeling of Friction Stir Welding, Journal of Materials Processing Technology, **171**, 348-357 (2006).

[16] O. Frigaard, O. Grong, O. T. Midling, A process model for friction stir welding of age hardening aluminum alloys, Metallurgical and Materials Transactions A – Physical Metallurgy and Materials Science **32**, 1189-1200 (2001).

[17] T. Sato, D. Otsuka, Y. Watanabe, Designing of Friction Stir Weld Parameters with Finite Element Flow Simulation, Proceedings of the 6th International Symposium on Friction Stir Welding, Montreal, Canada, October 10-13, 2007.

[18] T. S. Srivatstan, V. K. Vasudevan, Tensile deformation and fracture-behavior of 7150-T77511 aluminum-alloy, Metals Materials and Processes **6**, 97-106 (1994).

[19] M. W. Mahoney, C. G. Rhodes, J. G. Flintoff, R. A. Spurling, W. H. Bingel, Properties of friction-stir-welded 7075 T651 aluminum, Metallurgical and Materials Transactions A – Physical Metallurgy and Materials Science **29**, 1955-1964 (1998).

[20] Y. S. Sato, H. Kokawa, K. Ikeda, M. Enomoto, S. Jogan, T. Hashimoto, Microtexture in the friction-stir weld of an aluminum alloy, Metallurgical and Materials Transactions A-Physical Metallurgy and Materials Science **32**, 941-948 (2001).

Received: 20 March 2008.